Electronic Supplementary Information

Cu$_2$O@Fe-Ni$_3$S$_2$ nanoflower *in-situ* grown on copper foam at room temperature as excellent oxygen evolution electrocatalyst

Li Li Wu, Yu Xian Yang, Xiao Hui Chen, Juan Luo, Hong Chuan Fu, Li Shen, Hong Qun Luo*, Nian Bing Li *

School of Chemistry and Chemical Engineering, Southwest University, Chongqing 400715, People's Republic of China

[*]Corresponding author.

Hong Qun Luo and Nian Bing Li

*E-mail address: luohq@swu.edu.cn; linb@swu.edu.cn

Tel: +86-23-68253237

Experimental materials

Hydrochloric acid (HCl, AR) and ethanol (C$_2$H$_5$OH, AR) were purchased from Chongqing Chuandong Chemical Co., Ltd. (China). Nickel(II) chloride hexahydrate (NiCl$_2$•6H$_2$O, AR), iron(III) chloride (FeCl$_3$, 99%), ascorbic acid (AR), sodium hydroxide (NaOH, AR), ammonium peroxydisulfate ((NH$_4$)$_2$S$_2$O$_8$, AR), and sodium thiosulfate pentahydrate (Na$_2$S$_2$O$_3$•5H$_2$O, AR) were obtained from Shanghai Titan Technology Co., Ltd. (China). Iridium oxide powder (RuO$_2$, 99%, Sigma-Aldrich) and nafion D-521 solution (5% w/v, Alfa Aesar) were bought from Sigma-Aldrich Chemical Reagent Co., Ltd.

Synthesis of Cu(OH)$_2$ nanorod array

All the experiments were carried out at 25℃.

A piece of Cu foam with the size of 1 ×3 cm^{-2} was cleaned with 3 M HCl solution, ethanol and deionized water for 10 min in turn. The pretreated Cu foam was soaked into 30 mL of aqueous solution containing 0.3 M (NH$_4$)$_2$S$_2$O$_8$ and 4 M NaOH for 5 min. Then, the light blue Cu foam was removed from the solution, washed several times with deionized water and ethanol, and dried in the oven at 60 ℃.

Synthesis of Cu$_2$O nano-polyhedron

The Cu(OH)$_2$ nanorod array was soaked into 30 mL of 0.6 M ascorbic acid solution for 30 min. Then, the orange-red foam was removed from the solution, washed several times with deionized water and ethanol, and dried at 60 ℃ in the oven.

Synthesis of Cu$_2$O@Ni$_3$S$_2$ nanocomposite

400 mg of NiCl$_2$•6H$_2$O was added to 20 mL of water/ethanol mixed solvent (v/v=1:1). After

ultrasonic dissolution, the dried Cu_2O nano-polyhedron and 12 mL of 2 M $Na_2S_2O_3\cdot5H_2O$ were added to the solution successively for 4 h. Then, the $Cu_2O@Ni_3S_2$ was removed from the solution, washed several times with deionized water and ethanol, and dried at 60 ℃ in the oven.

Synthesis of $Cu_2O@Fe\text{-}Ni_3S_2$ nanoflower

50 mg of $FeCl_3$ and 400 mg of $NiCl_2\cdot6H_2O$ were added to 20 mL water/ethanol mixed solvent (v/v=1:1), and the following steps were the same as those of $Cu_2O@Ni_3S_2$ synthesis.

Synthesis of $Fe\text{-}Cu_2O$ electrode

A portion of $FeCl_3$ (50 mg) was added to 20 mL water/ethanol mixed solvent (v/v=1:1), and the following steps were the same as the synthesis of $Cu_2O@Ni_3S_2$.

Synthesis of RuO_2 electrode

To obtain the RuO_2 electrode, 2 mg of RuO_2 powder was dispersed into a mixture solution containing 0.01 mL of Nafion solution, 0.19 mL of deionized water, and 0.05 mL of ethanol. After ultrasonicated for 30 min, a homogeneous ink was obtained. Then, 0.01 mL of the ink was coated onto a piece of cleaned Cu foam, and evaporated slowly under infrared lamp at room temperature.

Electrochemical characterization

All electrochemical tests were performed at room temperature through an electrochemical station (CHI660E, Shanghai Chenhuain, China). During the electrochemical process, a three-electrode system was formed by utilizing the prepared sample, graphite rod, and saturated Ag/AgCl electrode as the working electrode, counter electrode and reference electrode, respectively. The polarization curves were obtained through linear sweep voltammetry (LSV) at a sweep rate of 5 mV s^{-1}. Electrochemical impedance spectroscopy (EIS) was carried out with frequencies ranging

from 0.01 Hz to 100 KHz and an amplitude of 10 mV. To estimate the electrocatalytic active surface area (ECSA) through the double-layer capacitance, cyclic voltammetry (CV) curves were collected in the potentials from 1.123 to 1.223 V vs RHE at different scan rates. All of the potentials vs. Ag/AgCl were converted to RHE via the Nernst equation ($E_{(vs\ RHE)} = E_{(vs\ Ag/AgCl)} + 0.059\ \text{pH} + 0.197$). IR compensation was utilized for all linear sweep voltammetry curves.

Characterization

A scanning electron microscope (SEM, LEO 1525) was utilized to detect the nanostructure and morphology. An energy dispersive X-ray spectroscope (EDX) was utilized to detect the elemental composition. A transmission electron microscope (TEM, JEOL JEM 2100F) was used to record the crystal structure. An X'Pert PRO diffractometer was utilized to detect the pattern of the X-ray diffraction (XRD) with Cu Kα radiation ($\lambda = 0.15406$ nm) at a scanning rate of 10 ° min^{-1}. The chemical states of catalyst were detected using an X-ray photoelectron spectroscope (XPS, Thermo Scientific K-Alpha+).
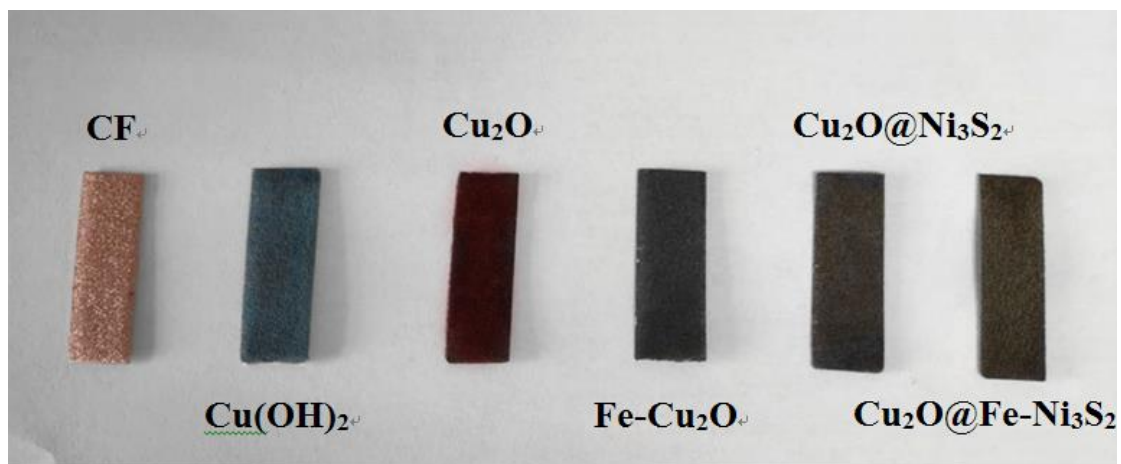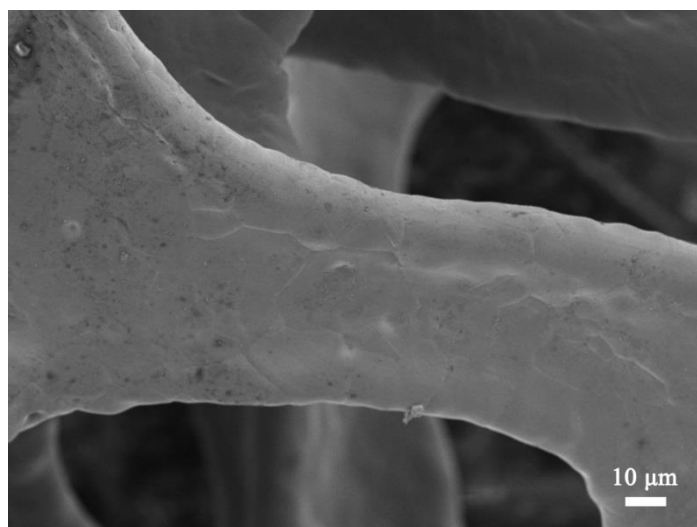
Fig. S1. Optical photograph of as-prepared samples.
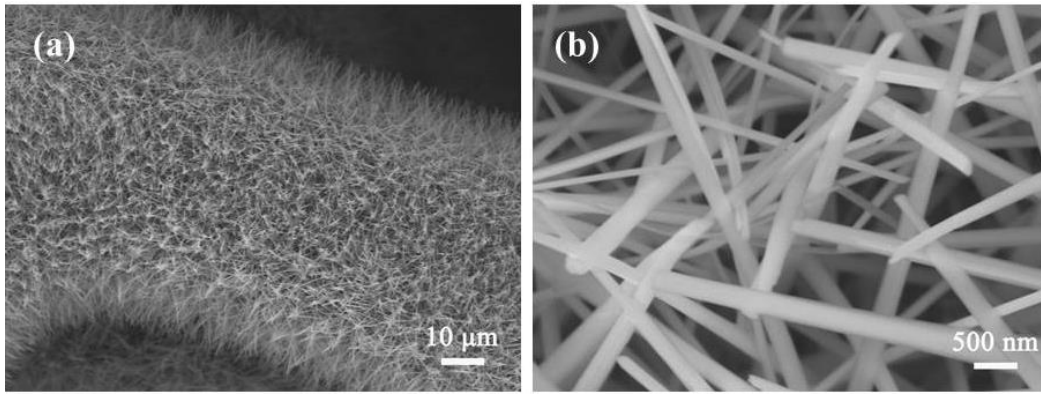

Fig. S2. SEM image of commercial Cu foam.
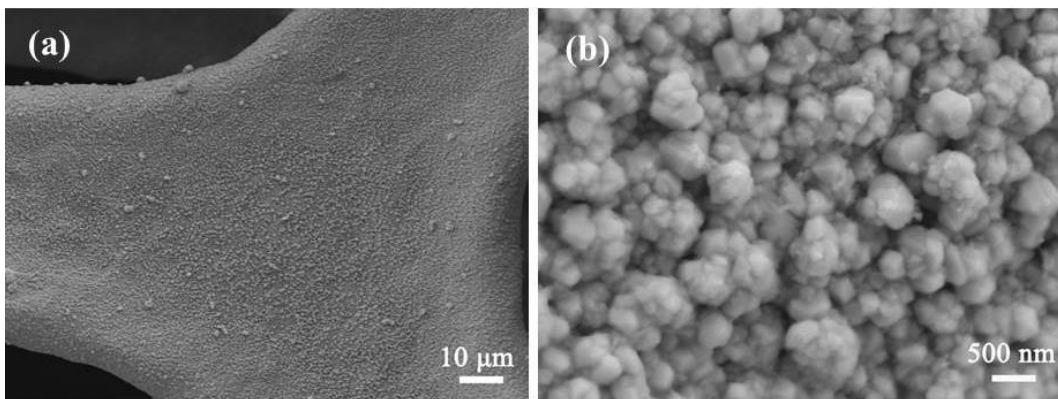
Fig. S3. SEM images of Cu(OH)$_2$.

Fig. S4. SEM images of Cu$_2$O.
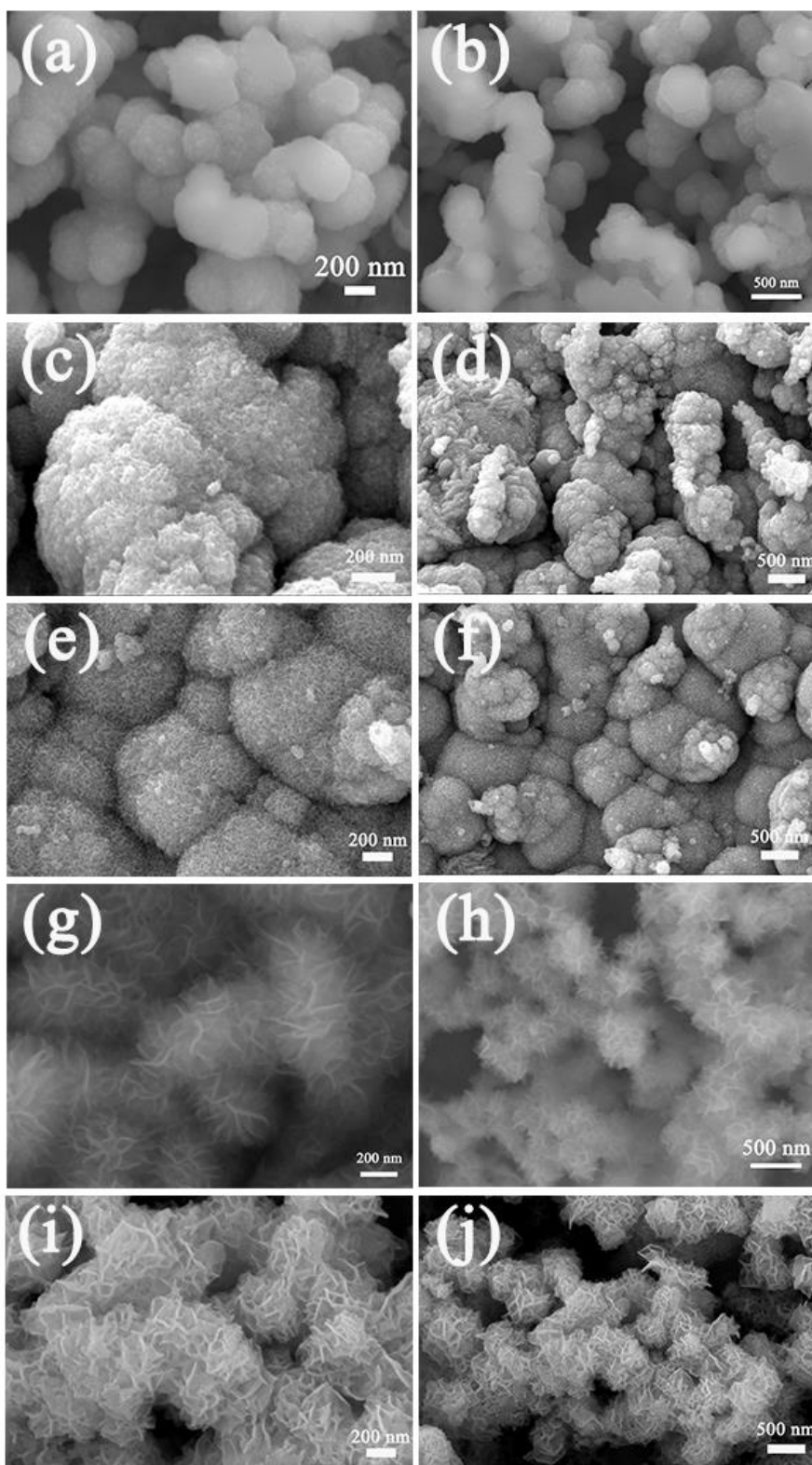
Fig. S5. SEM images of (a and b) $Cu_2O@Ni_3S_2$ (Fe/Ni=0:1), (c and d) $Cu_2O@Fe-Ni_3S_2$ (Fe/Ni=0.05:1), (e and f) $Cu_2O@Fe-Ni_3S_2$ (Fe/Ni=0.1:1), (g and h) $Cu_2O@Fe-Ni_3S_2$ (Fe/Ni=0.2:1), (i and j) $Cu_2O@Fe-Ni_3S_2$ (Fe/Ni=0.3:1) at different magnification.
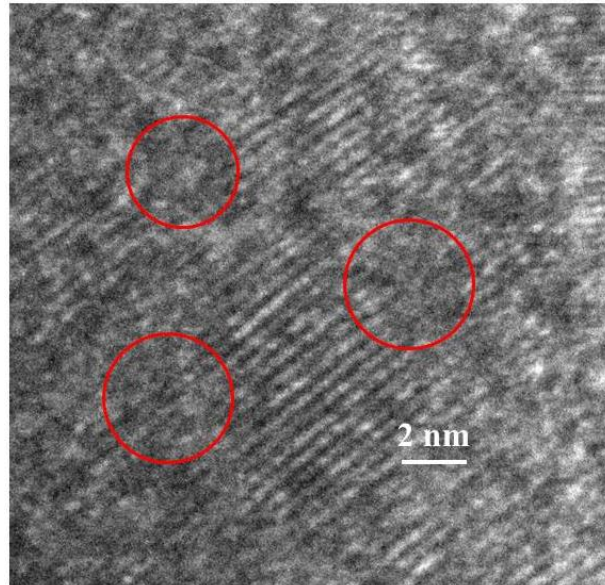
Fig. S6. HR-TEM image of the $Cu_2O@Fe-Ni_3S_2$. The red color represents the defect.

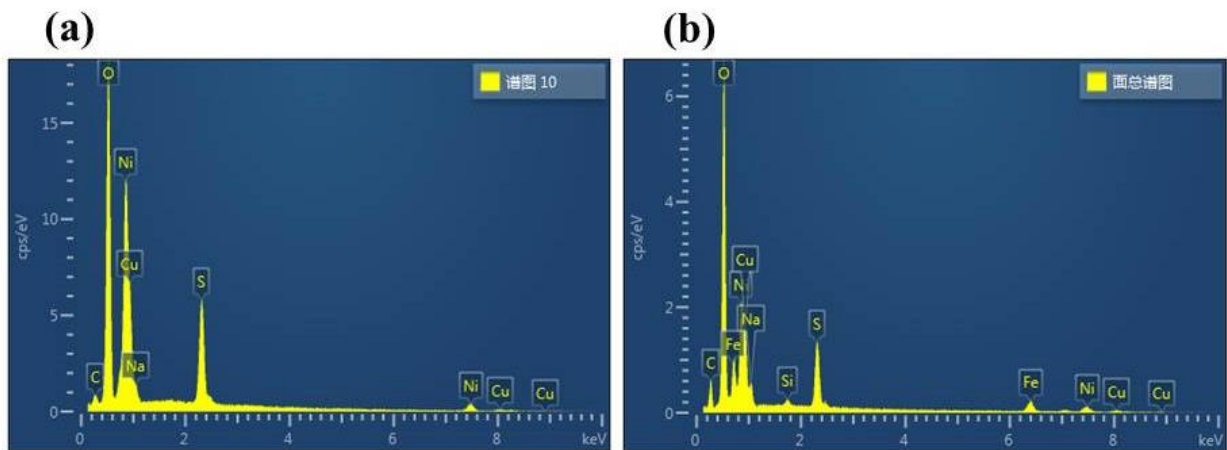**Fig. S7**. EDS characterizations of (a) $Cu_2O@Ni_3S_2$ and (b) $Cu_2O@Fe-Ni_3S_2$.

Table S1. Element contents of Ni, Fe and S in the EDS.

Sample	Ni (Atomic %)	S (Atomic %)	Fe (Atomic %)	Ni/S ratio	Fe/Ni ratio
$Cu_2O@ Ni_3S_2$	23.2	10.8	-	2.15	-
$Cu_2O@Fe-Ni_3S_2$	14.7	5.0	7.5	2.94	0.51
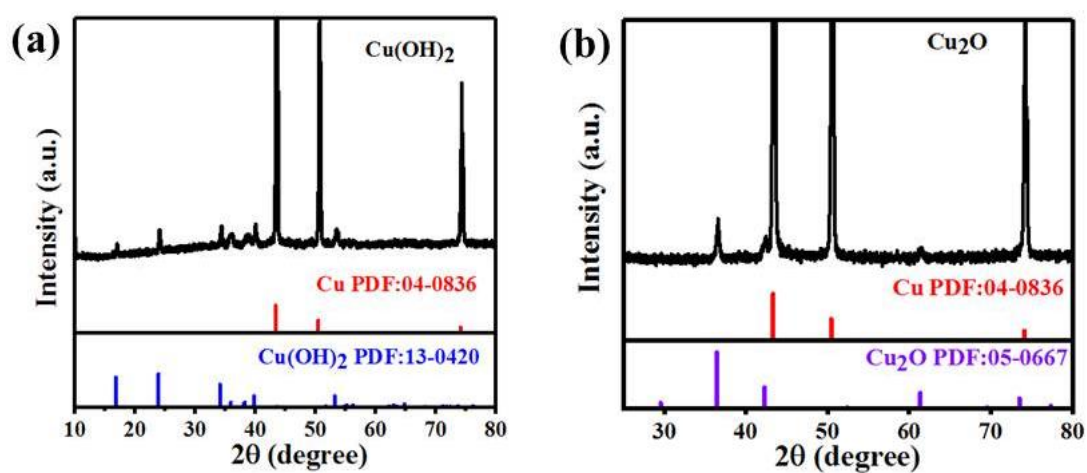
Fig. S8. XRD patterns of (a) $Cu(OH)_2$ and (b) Cu_2O.
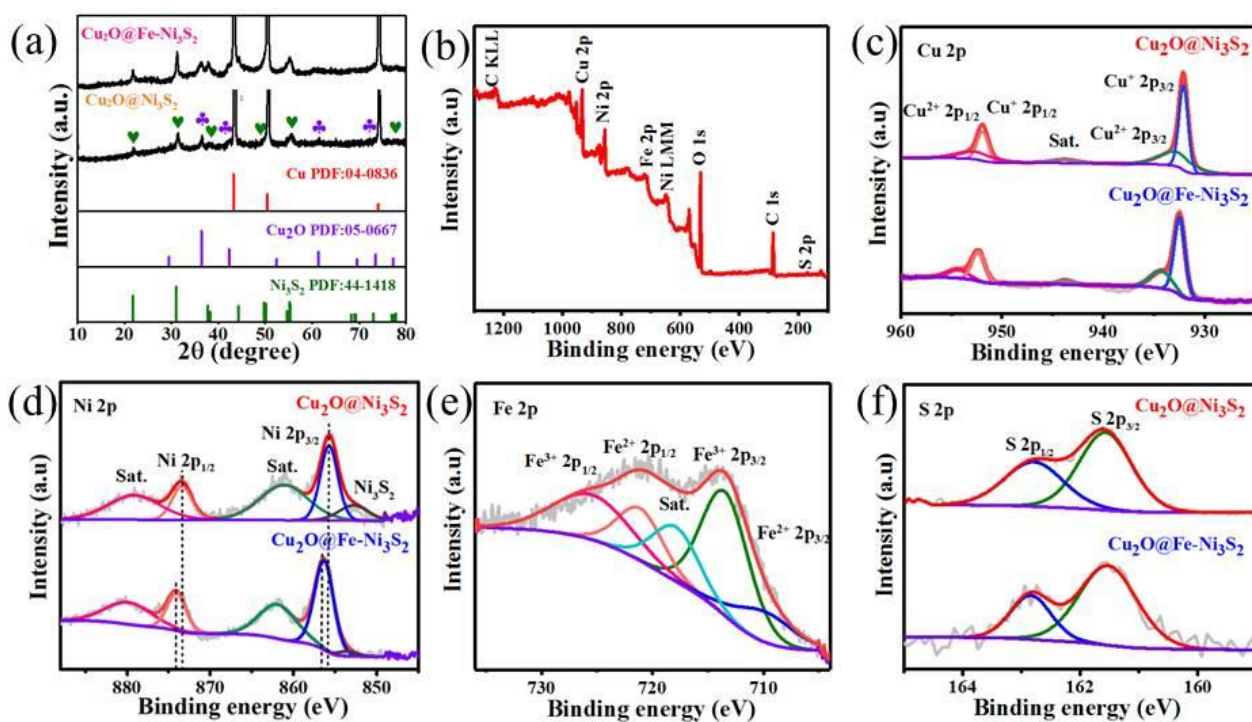
Fig. S9. (a) XRD patterns of $Cu_2O@Ni_3S_2$ and $Cu_2O@Fe-Ni_3S_2$. (b) The XPS full spectrum of $Cu_2O@Fe-Ni_3S_2$, and high-resolution XPS spectra of (c) Cu 2p, (d) Ni 2p, (e) Fe 2p, and (f) S 2p for $Cu_2O@Ni_3S_2$ and $Cu_2O@Fe-Ni_3S_2$.

Table S2. The peak area ratios of (S $2p_{3/2}$):(S $2p_{1/2}$) derived from the XPS spectra.

Sample	(S $2p_{3/2}$):(S $2p_{1/2}$)
$Cu_2O@\ Ni_3S_2$	1.70
$Cu_2O@Fe-Ni_3S_2$	2.07
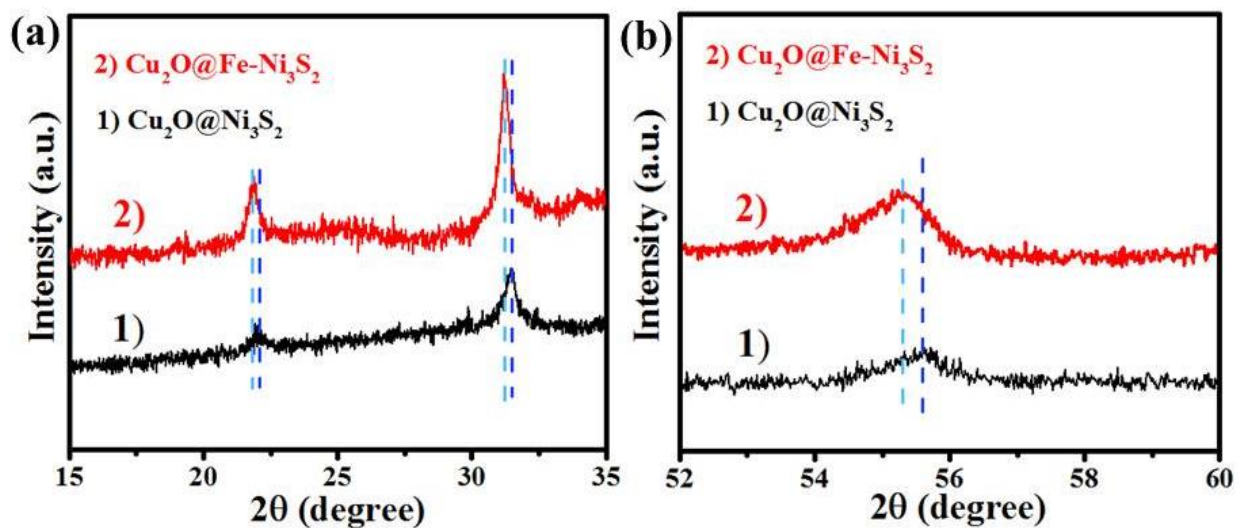
Fig. S10. (a and b) XRD patterns of $Cu_2O@Ni_3S_2$ and $Cu_2O@Fe-Ni_3S_2$.
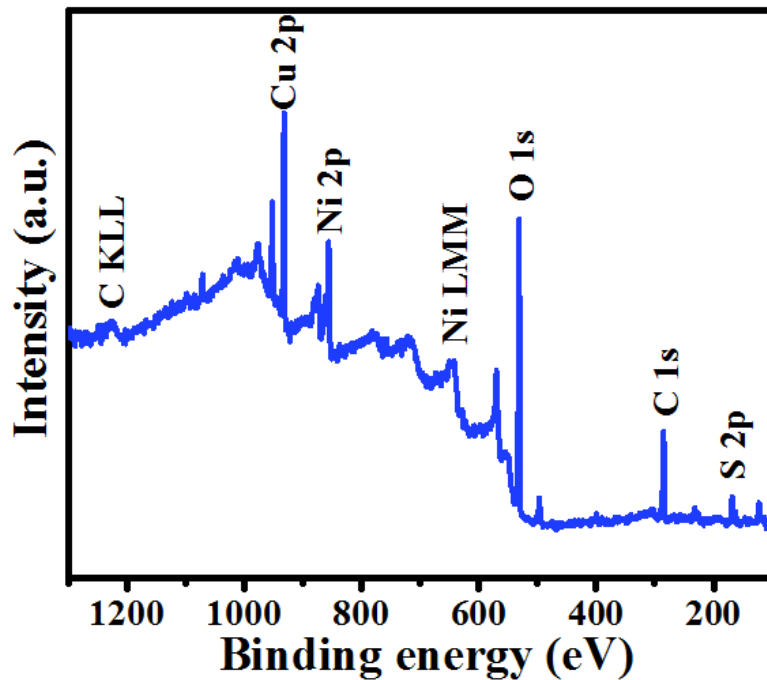

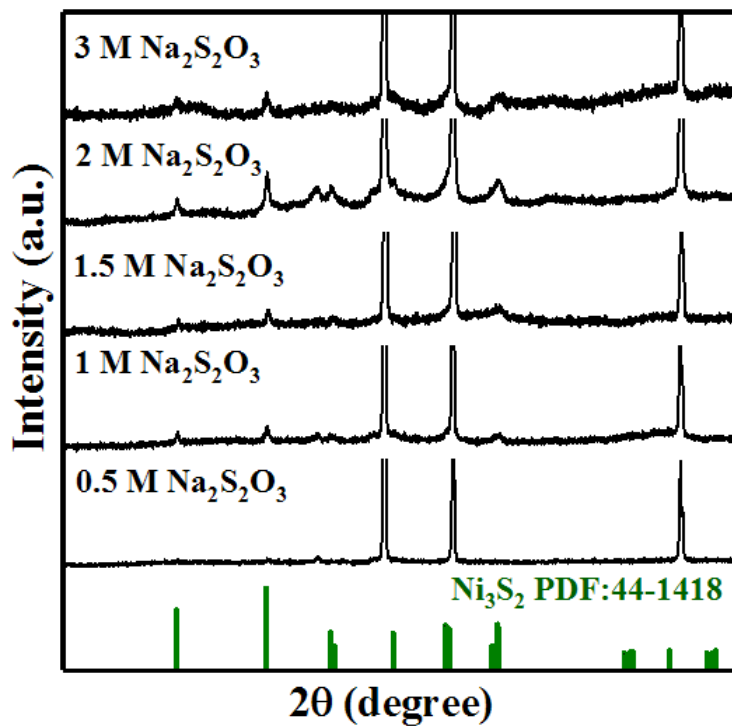**Fig. S11**. XPS full spectrum of $Cu_2O@Ni_3S_2$.

Fig. S12. XRD patterns of $Cu_2O@Fe-Ni_3S_2$ in the $Na_2S_2O_3$ solution with different concentrations.
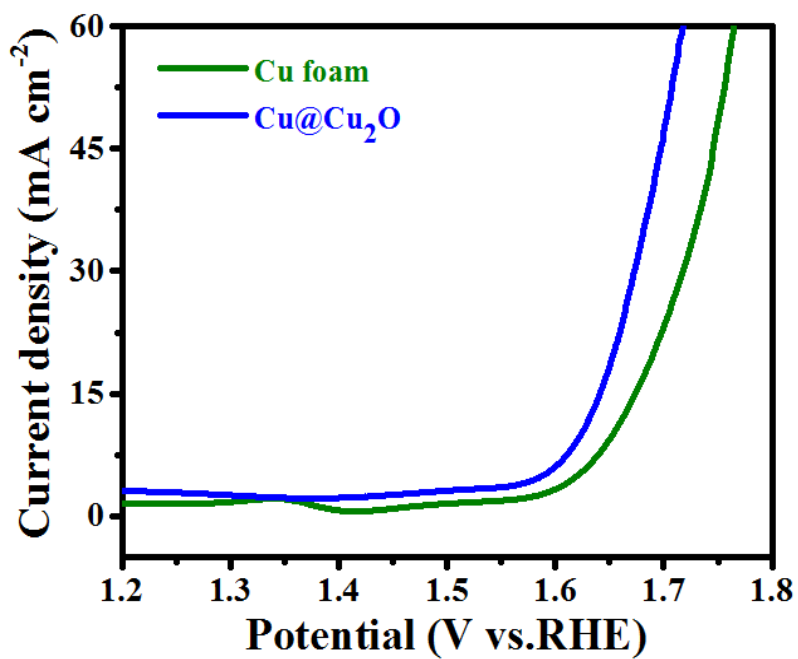

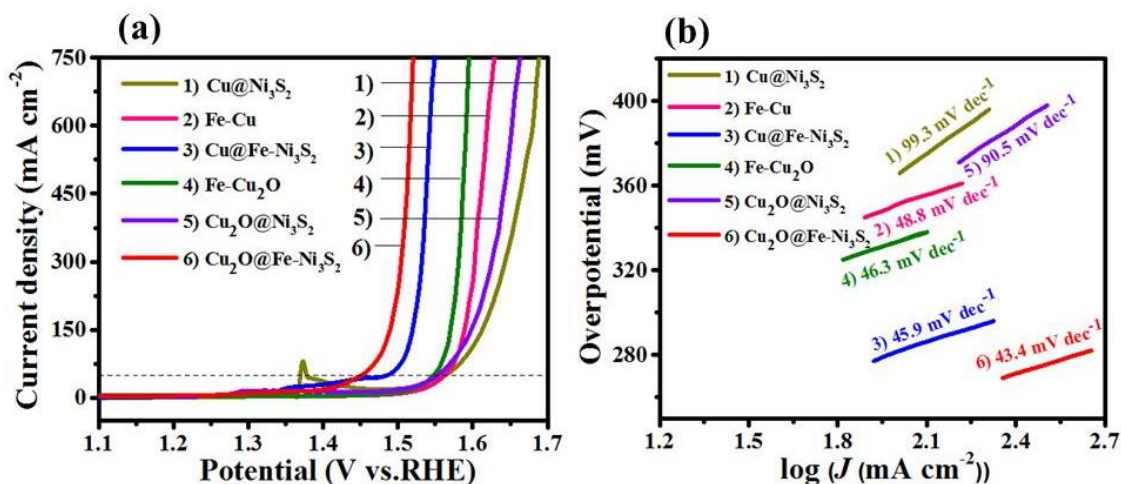**Fig. S13**. Polarization curves of Cu foam and $Cu@Cu_2O$ electrodes.

Fig. S14. (a) Polarization curves and (b) the Tafel plots of $Cu@Ni_3S_2$, Fe-Cu, $Cu@Fe-Ni_3S_2$, Fe-Cu_2O, $Cu_2O@Ni_3S_2$ and $Cu_2O@Fe-Ni_3S_2$ electrodes. (Preparation of $Cu@Ni_3S_2$, Fe-Cu and $Cu@Fe-Ni_3S_2$: Cu_2O was replaced by copper foam, and the other experimental conditions were consistent with those for $Cu_2O@Ni_3S_2$, Fe-Cu_2O and $Cu_2O@Fe-Ni_3S_2$, respectively.)
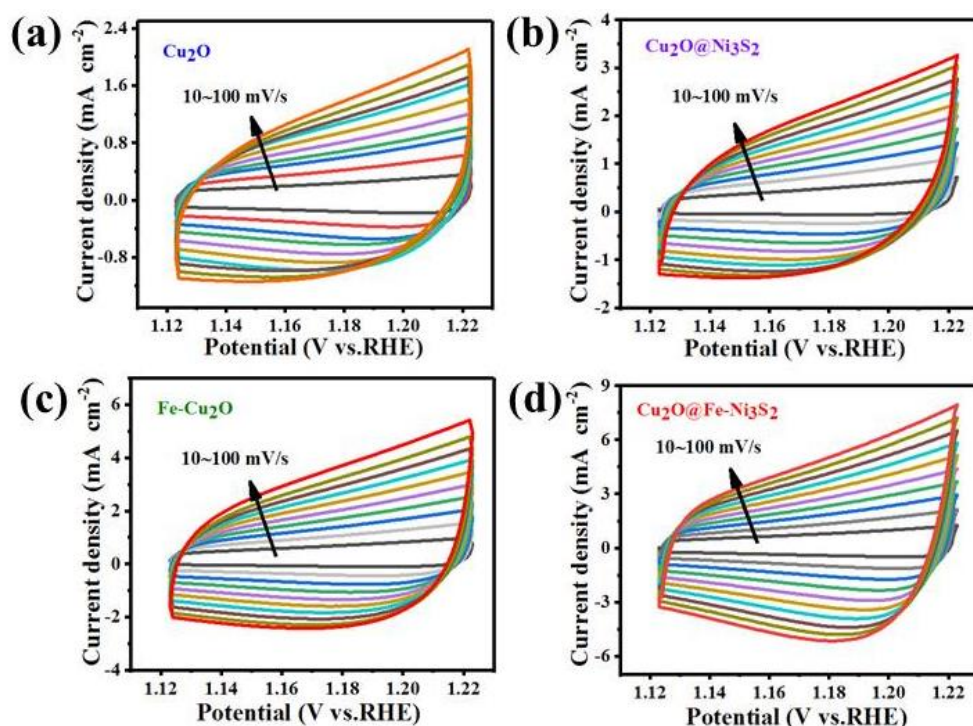
Fig. S15. Cyclic voltammograms of (a) Cu_2O, (b) $Cu_2O@Ni_3S_2$, (c) Fe-Cu_2O, and (d) $Cu_2O@Fe-Ni_3S_2$ at different scan rates ranging from 10 to 100 mV s^{-1} with an interval rate of 10 mV s^{-1}. The scanning potential range is from 1.123 to 1.223 V vs. RHE.
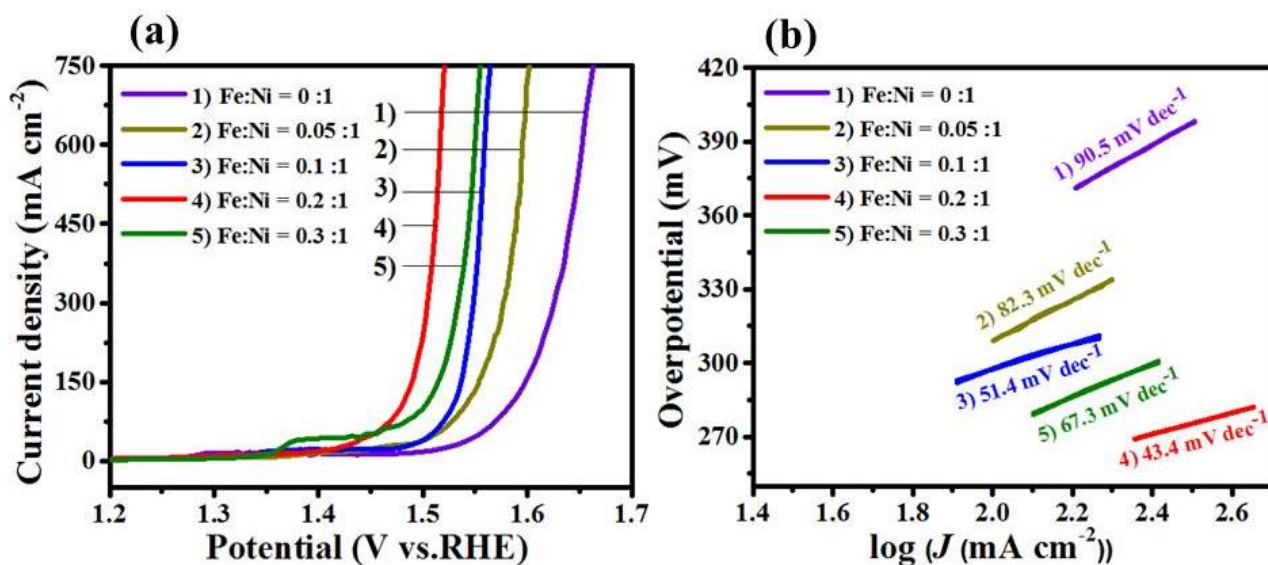
Fig. S16. (a) Polarization curves with iR correction and (b) corresponding Tafel plots of Cu$_2$O@Fe-Ni$_3$S$_2$ at different Fe/Ni feeding ratios. (Preparation of Cu$_2$O@Fe-Ni$_3$S$_2$: x mg of FeCl$_3$ (x = 0, 13, 25, 50 and 80) and 400 mg of NiCl$_2$•6H$_2$O were added to 20 mL of water/ethanol mixed solvent (v/v = 1:1), and the following steps were the same as those of Cu$_2$O@Ni$_3$S$_2$ synthesis.)
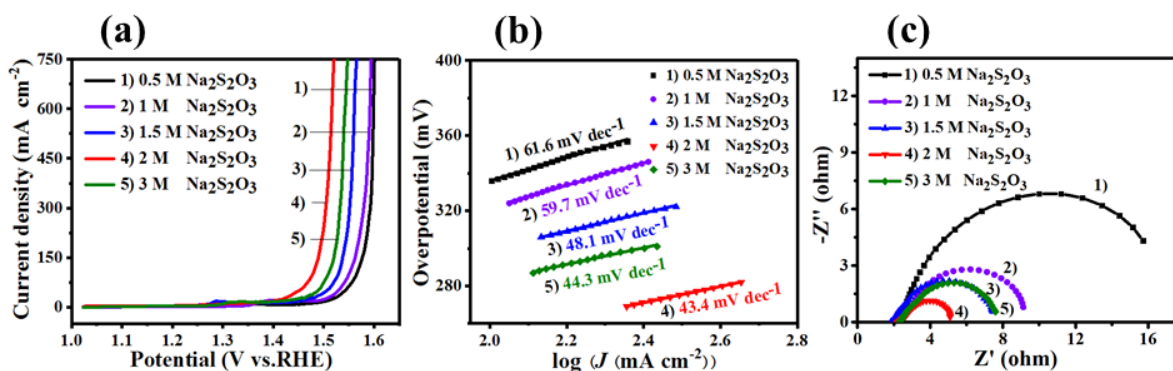
Fig. S17. (a) Polarization curves with iR correction, (b) corresponding Tafel plots and (c) EIS Nyquist plots of Cu$_2$O@Fe-Ni$_3$S$_2$ at different Na$_2$S$_2$O$_3$ concentrations.

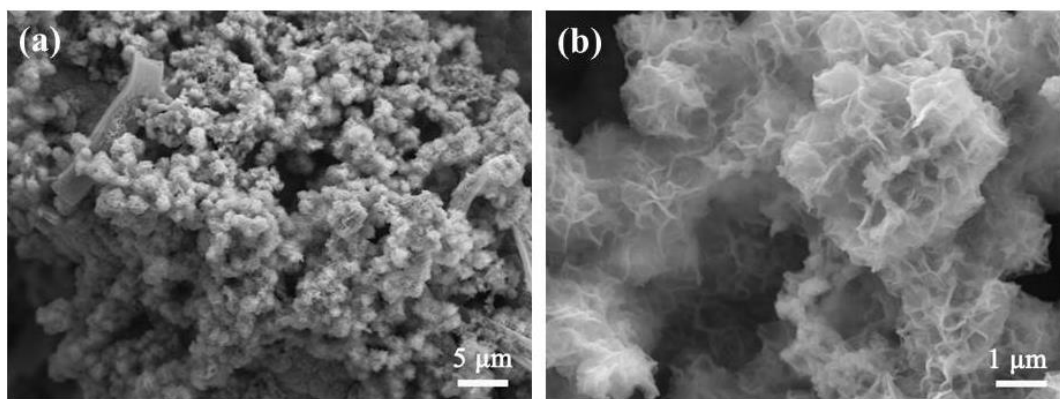**Fig. S18**. (a and b) SEM images of $Cu_2O@Fe\text{-}Ni_3S_2$ after OER stability test.

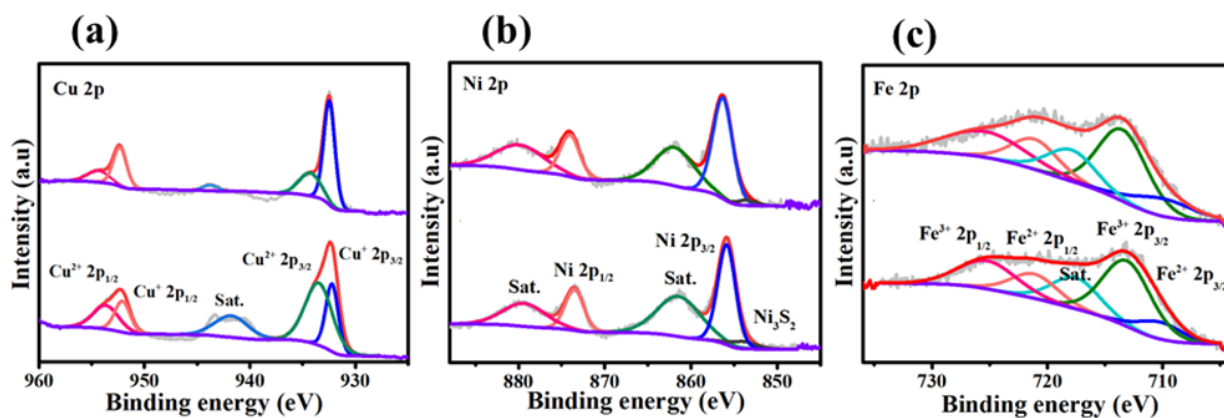**Fig. S19**. High-resolution XPS spectra of (a) Cu 2p, (b) Ni 2p, and (c) Fe 2p for $Cu_2O@Fe\text{-}Ni_3S_2$ before (up) and after (down) OER stability test.
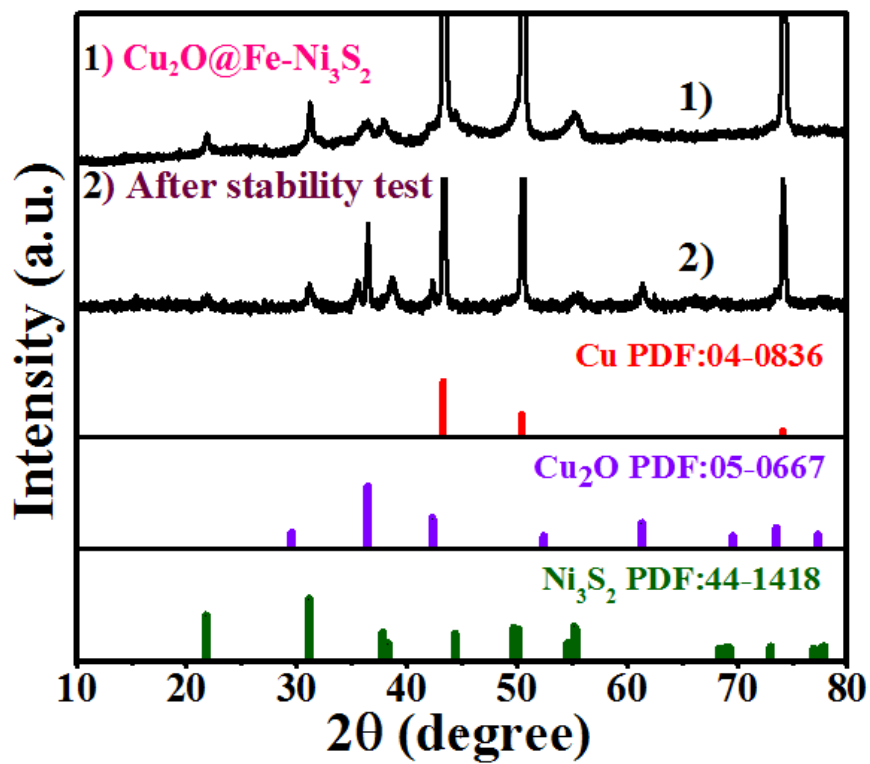
Fig. S20. XRD patterns of $Cu_2O@Fe-Ni_3S_2$ (1) before and (2) after OER stability test.

Table S3. Comparison of OER performance between $Cu_2O@Fe-Ni_3S_2$ and other Ni_3S_2-incorporated electrocatalysts reported in 1 M alkaline electrolyte.

Catalyst	η_{10} (mV)	η_{50} (mV)	η_{100} (mV)	η_{300} (mV)	Tafel slope (mV dec^{-1})	Ref.
$Cu_2O@Fe-Ni_3S_2$	NA	222	249	265	43.4	This work
$Sn-Ni_3S_2/NF$	NA	NA	260	360	52.7	[1]
$MoS_2-Ni_3S_2$ HNRs[a]/NF	249	NA	340	396	57	[2]
$Ni_2P/Ni_3S_2/NF$	210	NA	290	387	62	[3]
$V-Ni_3S_2@NiFe$ LDH[b]	209	NA	286	329	32.5	[4]
$Ni_xCo_{3-x}S_4/Ni_3S_2/NF$	160	NA	330	NA	95	[5]
$Ni_3S_2/NF-4$	242	NA	NA	NA	74	[6]
$CuCo-Ni_3S_2/NF$	NA	NA	400	NA	94.9	[7]
$V-Ni_3S_2/CC$	180	NA	NA	NA	56	[8]
$Fe-2-Ni_3S_2/rGO^c@NF-120$	NA	273	NA	NA	63	[9]
$TiO_2@Ni_3S_2$	220	NA	300	NA	NA	[10]
$Mo_xW_{1-x}S_2@Ni_3S_2/NF$	285	NA	NA	NA	90	[11]
$Zn-Ni_3S_2/NF$	NA	NA	330	NA	87	[12]
$N-Ni_3S_2/NF$	NA	NA	330	NA	70	[13]
MoS_2/Ni_3S_2	218	NA	NA	NA	88	[14]
$CoMoS_4/Ni_3S_2$	200	NA	NA	NA	63	[15]

a: heteronanorods   b: layered double hydroxide   c: reduced graphene oxide

References

1. J. Jian, L. Yuan, H. Qi, X. Sun, L. Zhang, H. Li, H. Yuan and S. Feng, *ACS Appl. Mater. Interfaces*, 2018, **10**, 40568-40576.

2. Y. Yang, K. Zhang, H. Lin, X. Li, H.C. Chan, L. Yang and Q. Gao, *ACS Catal.*, 2017, **7**, 2357-2366.

3. L. Zeng, K. Sun, X. Wang, Y. Liu, Y. Pan, Z. Liu, D. Cao, Y. Song, S. Liu and C. Liu, *Nano Energy*, 2018, **51**, 26-36.

4. J. Zhou, L. Yu, Q. Zhu, C. Huang and Y. Yu, *J. Mater. Chem. A*, 2019, **7**, 18118.

5. Y. Wu, Y. Liu, G-D. Li, X. Zou, X. Lian, D.Wang, L. Sun, T. Asefa and X. Zou, *Nano Energy*, 2017, **35**, 161-170.

6. J. Zhang, Y. Li, T. Zhu, Y. Wang, J. Cui, J. Wu, H. Xu, X. Shu, Y. Qin, H. Zheng, P.M. Ajayan, Y. Zhang and Y. Wu, *ACS Appl. Mater. Interfaces*, 2018, **10**, 31330-31339.

7. J-F. Qin, M. Yang, S. Hou, B. Dong, T-S. Chen, X. Ma, J-Y. Xie, Y-N. Zhou, J. Nan and Y-M. Chai, *Appl. Surf. Sc*i., 2020, **502**, 144172.

8. L. Ma, K. Zhang, S.Wang, L. Gao,Y. Sun, Q. Liu, J. Guo and X. Zhang, *Appl. Surf. Sci.*, 2019, **489**, 815-823.

9. D. Shao, P. Li, R. Zhang, C. Zhao, D. Wang and C. Zhao, *Int. J. Hydrogen Energy*, 2019, **44**, 2664-2674.

10. S. Deng, K. Zhang, D. Xie, Y. Zhang, Y. Zhang, Y. Wang, J. Wu, X. Wang, H.J. Fan, X. Xia and J. Tu, *Nano-Micro Lett*. 2019,**11**, 12.

11. M. Zheng, J. Du, B. Hou and C-L. Xu, *ACS Appl. Mater. Interfaces,* 2017, **9**, 26066-26076.

12. Q. Liu, L. Xie, Z. Liu, G. Du, M.A. Abdullah and X. Sun, *Chem. Commun.*, 2017, **53**, 12446-12449.

13. P. Chen, T. Zhou, M. Zhang, Y. Tong, C. Zhong, N. Zhang, L. Zhang, C. Wu and Y Xie*, Adv. Mater.*, 2017, **29**, 1701584.

14. J. Zhang, T. Wang, D. Pohl, B. Rellinghaus, R. Dong, S. Liu, X Zhuang and X. Feng, *Angew. Chem. Int. Ed.*, 2016, **55**, 6702-6707.

15. P. Hu, Z. Jia, H. Che, W. Zhou, N. Liu, F. Li and J. Wang, *J. Power Sources*, 2019, **416**, 95-103.